scientific reports

Check for updates

OPEN

A first-of-its-kind 3D biomimetic artificial mouth capable of reproducing the oral processing of soft foods

Alejandro Avila-Sierra[1]✉, Yurixy Bugarin-Castillo[1], Miodrag Glumac[1], Jérôme Bussiere[1], Anne Saint-Eve[1], Vincent Mathieu[2], Yoshikazu Kobayashi[3] & Marco Ramaioli[1]✉

With a growing global population and ageing demographics, the food industry stands at a pivotal crossroads, necessitating bespoke solutions and groundbreaking innovations. In vitro experiments can help understanding food oral processing and formulating products meeting the specific needs of different populations. However, current in vitro models do not reproduce well human oral anatomy and tongue biomechanics, essential for assessing the behaviour of novel and texturized foods under physiologically relevant oral conditions. In response, we unveil a novel 3D biomimetic artificial mouth, showcasing a pneumatic multi-degree-of-freedom artificial tongue meticulously crafted to mirror the mechanical properties and wettability of the human tongue. This cutting-edge technology, featuring tongue surface papillae, is capable of performing lifelike movements. The comparison with in vivo data demonstrates that it accurately reproduces oral processing of three, vastly different, soft foods. Textural characteristics (firmness, adhesive and cohesive properties) and shear viscosities—measured at oral and oropharyngeal-relevant shear rates—of in vitro food boli closely mirrored those observed in vivo. This in vitro device presents unprecedented opportunities for studying the dynamics of food transformation in the mouth, to adapt texture towards food that can be swallowed with ease and to improve food palatability, accommodating specific health needs critical for older adults (e.g., reduced salivary secretion, tongue weakness or poor coordination).

Keywords Artificial mouth, Biomimetic tongue, Food oral processing, Food texture, Ultrasound imaging, In vitro bolus

The global population is expected to grow by nearly 2 billion in the next three decades[1], along with a significant demographic transition. In developed economies, where one in six people will be over 65 years old[2], food industry challenges become notably heightened. Addressing these challenges requires developing healthier, more sustainable, and convenient food options. These alternatives are essential for promoting healthy ageing by facilitating the maintenance of healthy dietary patterns[3].

Presently, there is a stark scarcity of food products tailored for older adults[4], especially in mainstream supermarkets, where the majority (up to 97%) of them do their shopping[5]. This gap is evident when compared to the variety of food products available for other age groups like infants and children[4]. Developing food products for older consumers is challenging due to the multitude of factors influencing their eating experience, including diminished appetite[6], reduced taste and aroma perception[7,8], compromised oral motor functions[9], changes in texture perception[10,11], and swallowing difficulties[12,13]. Factors like reduced saliva production[14], tooth loss[15] and sarcopenia (progressive loss of muscle mass, strength, and function with ageing)[16] can also contribute to prolonged oral processing time, affecting appetite regulation[17–19]. This emphasises the unique dietary needs of older adults, often prioritising ease of consumption over nutritional content[4], for which food must be designed with specific nutritional compositions and physical properties to support their health and well-being.

During eating, liquids quickly undergo changes before swallowing, including heating, dilution, dissolution of water-soluble materials, and chemical breakdown facilitated by salivary enzymes[20–22]. In contrast, solid foods

[1]Université Paris-Saclay, INRAE, AgroParisTech, UMR SayFood, 91120 Palaiseau, France. [2]INRAE, Institut Agro, STLO, 35042 Rennes, France. [3]Department of Dentistry and Oral-Maxillofacial Surgery, School of Medicine, Fujita Health University, Toyoake, Aichi 470-1192, Japan. ✉email: alejandro.avila-sierra@inrae.fr; marco.ramaioli@inrae.fr

also require chewing to break down their structure[23]. Saliva, along with other fluid components like moisture and fats, helps lubricate this process[24]. Changes in food structure and lubrication persist throughout chewing until the food bolus is ready for swallowing[25,26].

Tailored feeding strategies for older adults or individuals with specific health conditions may involve thickening liquids or altering solid food textures, impacting eating habits and oral processing dynamics[27]. These changes can lead to prolonged processing times for thickened liquids and a shift from teeth-driven chewing to tongue-driven mechanical processing for textured foods[28,29]. Many elderly individuals, particularly those lacking natural teeth, may rely on tongue-based methods for breaking down and managing food[30], limiting their food choices due to reduced oral capabilities. The tongue, a soft skeletal muscle, typically exerts a maximum compressive force of up to 70 kPa against the palate[31]. However, age-related factors like sarcopenia can reduce tongue pressure[32], complicating oral processing further.

Recent progress in developing bio-inspired and biomimetic in vitro systems has advanced our understanding of food oral processing, especially when chewing hard solid foods[33,34]. These systems replicate the human masticatory system to analyse the effects of occlusal forces, movements, and salivary lubrication on food bolus characteristics[35,36]. However, they lack integration of the tongue, essential for breaking down and mixing food, particularly when consuming textured or very soft food. Most studies on semi-solid or soft foods use uniaxial compression experiments to simulate the compression action akin to that of the tongue against the palate[28,37]. While more advanced bio-inspired systems have emerged recently, featuring biomimetic tongue-like surfaces and user-customisable trajectories, these primarily serve tribological studies aimed at correlating interfacial friction with food mouthfeel rather than delving into the bolus formation process[38,39]. Consequently, none of the existing systems effectively capture the intricacies of oral anatomy and the physiological biomechanics of the human tongue, falling short of realistically simulating the dynamic changes occurring in the human oral cavity during food ingestion. In this dynamic process, tongue movements such as compression, smooth side-to-side motions, rolling actions, and anterior-posterior movements are known to play a pivotal role in breaking down food particles and homogenising them with saliva to form a suitable food bolus before swallowing.

In this study, we introduce a novel 3D biomimetic artificial mouth, showcasing a pneumatic multi-degree-of-freedom artificial tongue meticulously crafted to mirror the mechanical properties and wettability of the human tongue. This cutting-edge technology accurately mimics lifelike movements and reproduces the structures of tongue surface papillae, faithfully imitating the primary tongue motions observed in vivo during oral processing of soft foods of various consistencies. Through comprehensive characterisation of the model foods, including textural and rheological assessments, we systematically compared these attributes between in vivo and in vitro food boli ready for swallowing. This innovative in vitro device provides unparalleled insights into the dynamics of food transformation in the mouth and holds significant promise in enhancing food palatability and functionality, offering valuable contributions to research and practical applications in human nutrition and health.

Results

Characterisation of model foods

Three commercial products, denoted as Viscous Liquid (VL), Aerated Soft Solid (ASS), and Soft Solid (SS), were chosen as model foods due to their diverse textural consistencies—cream, mousse, and gel-like respectively. A comprehensive characterisation of the model foods is included in Fig. 1a. ANOVA analysis is detailed in Supplementary Table SI.1.

The moisture content analysis revealed distinct water levels ($p < 0.05$) among them, with ASS exhibiting the lowest ($64.7 \pm 0.2\%$) and SS the highest ($75.2 \pm 0.2\%$). The textural characteristics of these products, including firmness, compression work, adhesion work, and maximum adhesion force, were explored due to their potential to impact on food oral processing and their interactions with pertinent oral surfaces. As expected, VL was the most easily spreadable food (firmness 44.9 ± 1.8 N.s), requiring less compression work for initial deformation (2.8 ± 0.2 N). In contrast, ASS exhibited the greatest resistance to initial deformation (firmness 99.3 ± 7.9 N.s), necessitating more than double the compression work compared to VL (7.9 ± 0.5 N). In terms of adhesive properties, VL and SS displayed similar levels ($p = 0.90$ and $p = 0.08$ for $W_{Adhesion}$ and $F_{Adh.\ Max}$, respectively). Notably, ASS exhibited over twice the adhesion work (-49.4 ± 6.8 N.s) and force (-7.3 ± 0.6 N) compared to other products, indicating a markedly stickier nature.

Rheological properties were also evaluated to analyse the flow resistance of the model foods. The shear viscosity profiles, depicting the relationship between shear rates (ranging from 1 to 1000 s^{-1}), are provided in Supplementary Fig. SI.1. All model foods exhibited shear thinning behaviours. At orally relevant shear rate (50 s^{-1})[40], both VL and ASS showed comparable flow abilities (1.1 ± 0.0 Pa.s and 1.4 ± 0.4 Pa.s, respectively; $p = 0.58$). In contrast, SS demonstrated significantly higher resistance to flow (2.1 ± 0.1 Pa.s), although not statistically different from ASS ($p < 0.06$) due to the higher variability between measurements observed for the sticky and aerated food. For SS, two similar shear thinning phases were observed, with a less pronounced shear thinning phase occurring between 50 and 100 s^{-1}.

Characterisation of ready-to-swallow food boli

Oral processing induces structural changes in ingested foods through the coordinated movements of the tongue, teeth, and cheeks, along with temperature fluctuations, dilution, and other chemical transformations facilitated by the salivary fluid[22]. This process aims to achieve a harmonious balance between the adhesive and cohesive properties of the resulting food bolus, ensuring its suitability for swallowing[25,26].

The model foods, previously characterised, were employed in in vivo sensory studies, wherein healthy adult panellists ($n = 3$) were instructed to perform oral processing—unrestricted oral conditions—until the moment of swallowing. At this juncture, the resultant food boli were expectorated and collected for characterisation (Fig. 1b). ANOVA analysis is detailed in Supplementary Table SI.1.

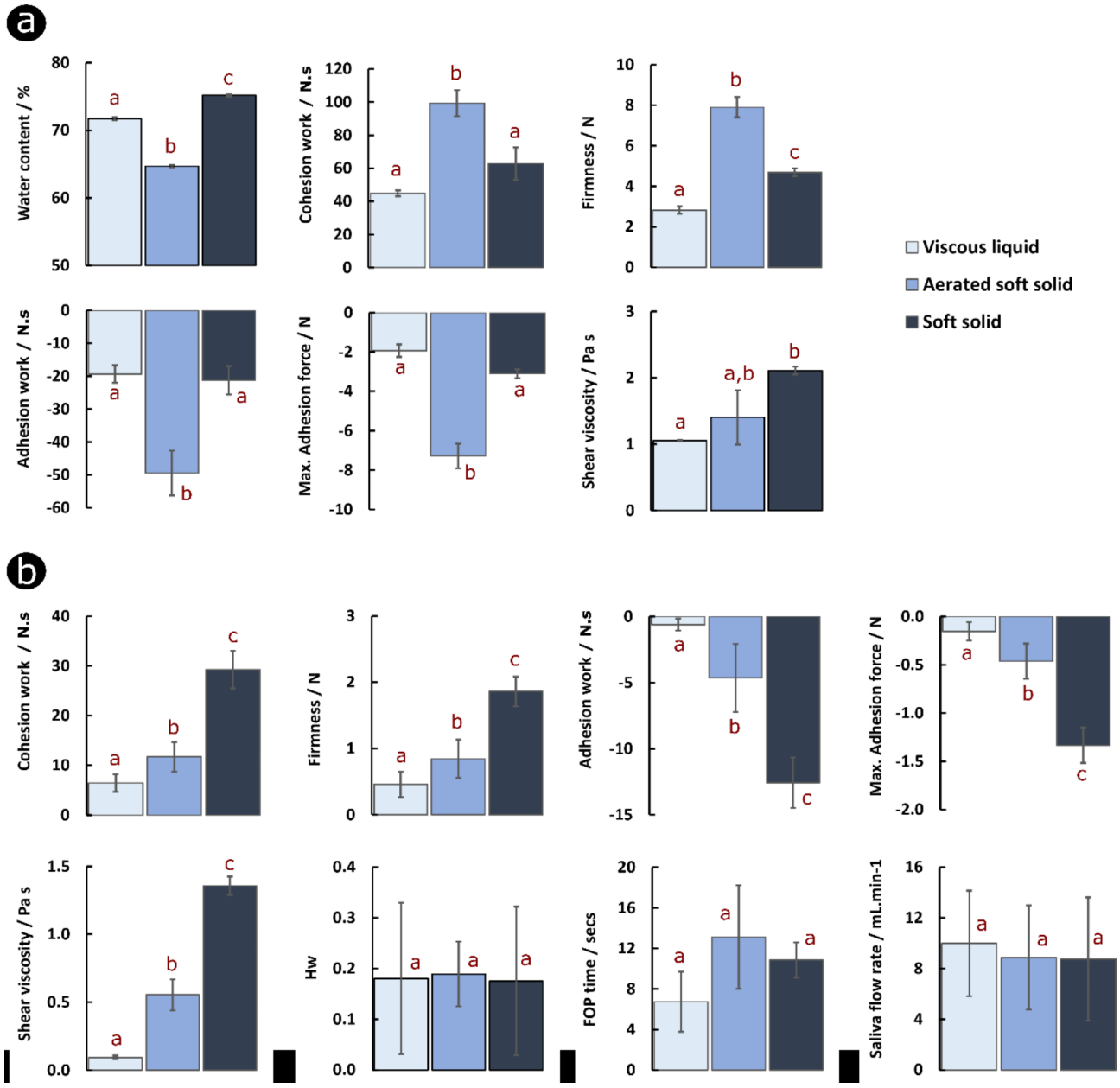

Fig. 1. Characterisation of (**a**) model foods and (**b**) ready-to-swallow in vivo food boli. The parameters analysed include water content, textural attributes (i.e., firmness, cohesion work, adhesion work, and maximum adhesive force), and shear viscosity at the relevant oral shear rate ($50s^{-1}$). Additional parameters such as insalivation ratio (H_w), food oral processing (FOP) time derived from US recordings ($n=10$), and the stimulated salivary flow rate are reported for in vivo food boli. Averaged data along with corresponding standard deviations are shown. Model foods were subjected to three repetitions ($n=3$), while food boli were analysed through three repetitions across three different panellists ($n=3\times3$). Statistical significance ($p<0.05$) between datasets is denoted by letters. Water content varied between foods, with ASS at the lowest and SS the highest. VL was the most spreadable, requiring less compression work (similar to SS), while ASS resisted the most, needing double the compression work compared to VL. Adhesion varied, having both VL and SS similar adhesive properties while ASS had over twice the adhesion work and force. At relevant oral conditions, VL and ASS showed similar flow abilities (1.1 and 1.4 Pa.s, respectively). SS exhibited higher resistance (2.1 Pa.s), featuring distinct shear thinning phases between 50–100 s^{-1} (shear viscosity profiles of both foods and boli are included in Supplementary Information). After oral processing, food boli spreadability improved, with over 80% firmness decrease for VL and ASS, and around 60% for SS. Compression effort reduced over 85% for VL and ASS, and approximately 50% for SS. Adhesion forces decreased by over 90% for VL and ASS, and approximately 60% for SS. This reduction contributed to a notable decrease in adhesion work, exceeding 90% for VL and ASS, and around 40% for SS. Flow resistance varied, with VL showing the most significant decrease to 0.1 Pa.s, followed by ASS with a 60% reduction and SS with a 36% decrease. Food-to-saliva ratio, FOP time, and estimated salivary flow rate showed no significant differences among food boli.

As anticipated, the textural properties of the formed food boli underwent substantial modifications compared to their original characteristics. The spreadability of the food boli demonstrated noteworthy improvements, with a firmness decrease exceeding 80% for VL and ASS, and approximately 60% for SS. This enhancement resulted in a significant reduction in the effort required for food compression, surpassing 85% for VL and ASS, and around 50% for SS. Moreover, a favourable decline in the adhesion forces initially associated with the food products was observed, exceeding 90% for VL and ASS, and approximately 60% for SS. This reduction significantly contributed to a notable decrease in the work of adhesion for the processed food, exceeding 90% for VL and ASS, and ~ 40% for SS.

The resistance to flow of the shear thinning food boli at the orally relevant shear rate (50 s^{-1}) also showed notable differences, being the most pronounced one the decrease observed for VL, with a shear viscosity plummeting from 1.2 ± 0.0 Pa.s to 0.1 ± 0.0 Pa.s (91% reduction). This was followed by ASS with a 60% reduction and SS with a comparatively lower decrease of 36%. In the case of SS, the shear viscosity decreased from 2.1 ± 0.1 Pa.s to 1.4 ± 0.1 Pa.s, indicating the least pronounced reduction among the samples.

Additional factors such as the insalivation ratio of food boli (H_w) and oral processing time (FOP time) were analysed to determine the extent of food product dilution, along with the potential impact that salivary enzymes may also have on food oral transformation. In terms of the food-to-saliva ratio, all boli exhibited a ratio of ~ 0.2 (20%), with no significant differences among them ($p = 0.98$), being consistent with the ratios reported for thickened liquids[41]. While FOP time varied based on the type of food (6.8 ± 3.0, 13.1 ± 5.1, and 10.9 ± 1.7 s for VL, ASS, and SS, respectively), the variability between individuals resulted in no statistical significance ($p = 0.26$). Both H_w and FOP time were used to estimate the stimulated salivary flow rate during oral processing. Despite a slightly higher saliva flow rate for VL (10.0 ± 4.2 mL/min) compared to ASS and SS (8.9 ± 4.1 mL/min and 8.8 ± 4.9 mL/min, respectively), no statistical differences were identified ($p = 0.84$). It is important to note that due to the short duration of FOP, the estimated stimulated flow rate might be influenced by the initial amount of saliva present in the mouth before introducing the food product, which could lead to a slight overestimation.

Deconstruction process of food intra-oral transformation

The act of consuming food is a dynamic process that evolves continuously until the moment of swallowing. To evaluate the predominant activities—compression, shearing, mixing, collection, mastication, and deglutition—and their timing in the mouth during food oral processing, Temporal Dominance of Motions (TDM) analysis[42] was employed during consumption of the three model foods. At a panel level ($n = 16$), Fig. 2 presents averaged TDM curves, illustrating the percentage of the citation rate of each activity being dominant as a function of the standardised time, along with representative Ultrasounds (US) images of a healthy panellist. These US images were used for qualitative analysis of the tongue movements performed during food consumption. Representative US recordings for each model food are included as Supplementary Material.

According to the results obtained with VL (Fig. 2a), up to approx. 55% of the participants initiated oral processing with a compressional tongue action. In this context, and according to US recordings, the action would be associated with transporting the liquid from the frontal to the mid part of the oral cavity to facilitate further food transformation (i–ii). This stage, involving the rising of the tongue tip and a depression of the tongue body, remained above the significance level for approximately 22% of the total duration of oral processing. Subsequently, most individuals (~ 35%) engaged in mixing (iii), occupying approximately 15% of the time. During mixing, the tongue moves the food product within the oral cavity to aid its mixing with saliva. This was followed by a stage dedicated to bolus collection. During this final stage, irrespective of the food tested, and prior to swallowing, food boli seem to be gathered at the back of the tongue through a squeezing-like motion of the tongue tip against the hard palate, transporting the food towards the posterior section of the tongue (iv)—as noted in clinical studies when consuming foods with varying consistencies[43].

During oral processing of ASS (Fig. 2b), an initial period of multiple compressions for altering the initial structure of the food product between the tongue and the hard palate (i–ii) takes precedence (40% of the time), being the dominant action for over 80% of the participants. This is succeeded by shearing (~ 15% of the time) generated between the tongue and the hard palate (iii), experienced by approximately 30% of individuals. Subsequently, participants execute a partial swallow of the food bolus, taking up 15% of the total time. Upon analysing US recordings, an initial partial swallow has been observed in 50% of the panellists ($n = 5$ out of 10). After a swift bolus collection action (iv), consuming about 5% of the time, the final swallow event is predominantly initiated.

Lastly, oral processing of SS (Fig. 2c) necessitated an initial compression period executed by over 80% of the participants, followed by a second compression period performed by approximately 50% of individuals (i–ii). Both periods of multiple compressions appear to account for about 34% of the total processing time. Subsequently, shearing (iii), lasting for ~ 7% of the time, was experienced by around 30% of the panellists during the second compression period, just before the collection of the food bolus (iv), which consumed 8% of the total time, leading to the initiation of the swallowing process.

In vitro simulation of food oral processing

To ensure an accurate replication of food oral processing in vitro, the primary actions identified in the preceding section, along with their respective time allocations throughout the process of food transformation, served as the basis for determining the timing ("Estimated in vivo time" and "Time per motion") of the in vitro sequence (see Table 1). This approach also helped in discerning the primary movements of the tongue (US images), considering the high variability of tongue actions between subjects during food oral processing. Consequently, a qualitative framework for designing the actuation pattern of the 3D biomimetic artificial tongue was established (Fig. 3). This framework incorporates a total of five tongue actions (Sect. 2.3): initial food displacement (a), compression

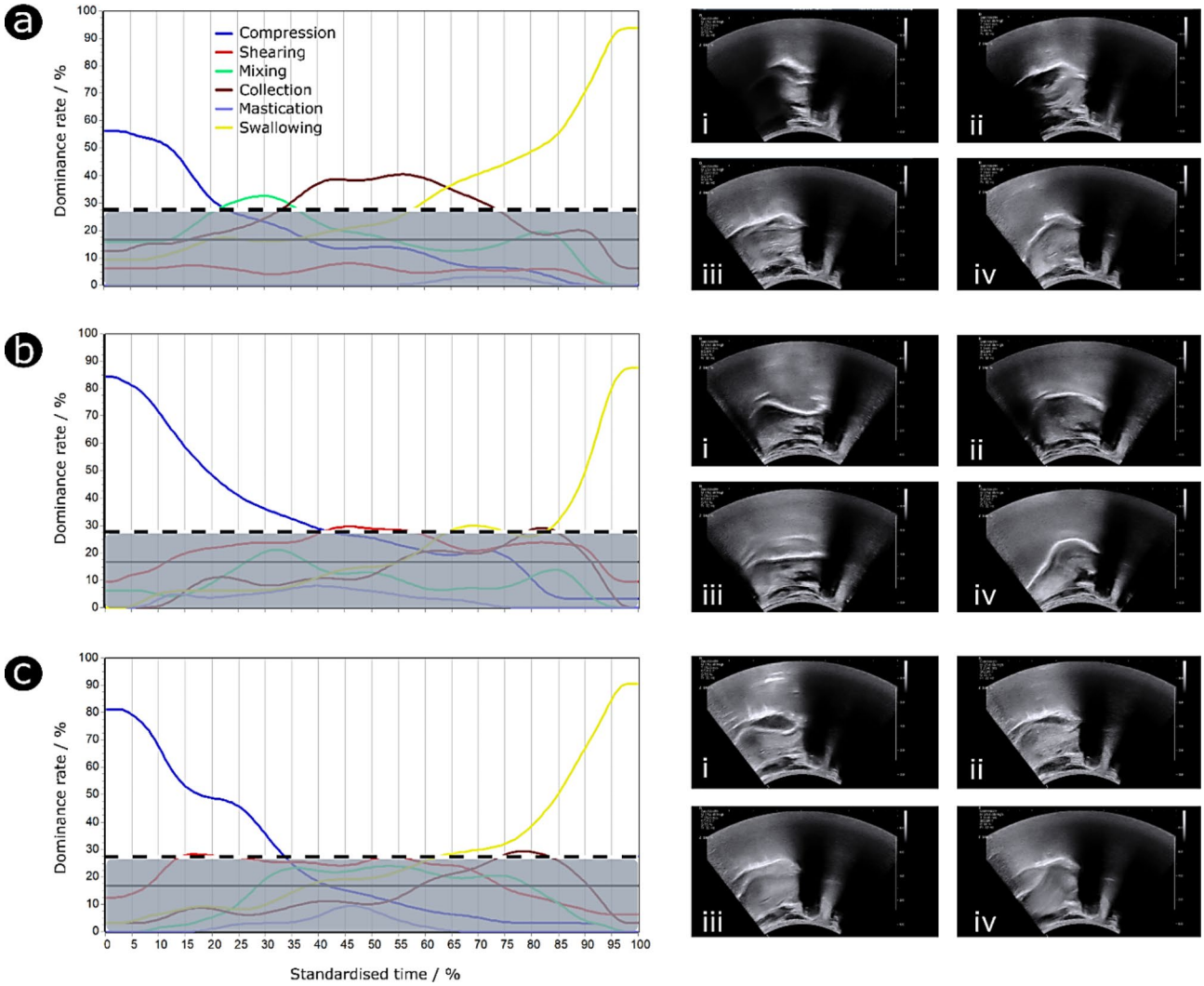

Fig. 2. Temporal dominance of motions (TDM) profiles illustrate the progression of actions during food oral processing over time, accompanied by representative Coronal plane US images depicting the predominant actions of the human tongue (tongue tip on the right) for various model foods, including (**a**) Viscous Liquid (VL), (**b**) Aerated Soft Solid (ASS), and (**c**) Soft Solid (SS). Actions above the dashed baseline indicate statistical significance (> 27.5%)[42,61], while actions within the shaded area signify no dominant significance. During VL oral processing (a), approximately 55% of participants initiated a compression-like phase associated with food displacement from the frontal to the mid part of the oral cavity (i–ii), accounting for about 22% of the total time. Subsequently, participants engaged in mixing the food with saliva (15% of time) (iii) before collecting and positioning the bolus within the oral cavity (iv) in preparation for the final swallow. For ASS (**b**), an initial phase of compressions of the food product between the tongue and hard palate prevailed (40% of time) (i–ii), followed by dominant shearing action (~ 15% of time) against the hard palate (iii). Approximately 30% of participants executed a partial swallow (15% of time), followed by swift bolus collection (5% of time) (iv), leading to the predominant initiation of the final swallow. In the case of SS (**c**), two initial compression periods accounted for about 34% of the total time (i–ii). During the second period, there was a representative shearing action (7% of time) (iii) just before food bolus collection (8% of time) (iv) to trigger the final swallow event.

of food and bolus (b), mixing of food bolus (c), shearing (d), and collection of the food bolus (e). For the in vitro simulation, the artificial tongue executes the following actions:

- Initial food displacement. The artificial tongue emulates this movement by adopting a depression-like shape, wherein the frontal air chamber remains unaffected while the lateral chambers deflate under vacuum (Fig. 3a, ii–iii).
- Food and bolus compression. The artificial tongue replicates this action by adopting a dome-like shape. In this configuration, the frontal air chamber remains inactive to ensure the product stays in the mid-frontal section of the oral cavity. Meanwhile, both lateral chambers inflate symmetrically (Fig. 3b, ii–iv), exerting the necessary compression force tailored to each type of product. The sagittal view (Fig. 3b, iv) illustrates the symmetrical inflation of the lateral chambers.

Dominant motion	Sequence order	Estimated in vivo time (s)	Number of motions	Time per motion/Total in vitro time (s)	Tongue pressure (kPa)	Palatal pressure (kPa)
Viscous liquid						
Food displacement	1st	2.6	1	2.6/2.6	NA*/− 3.4 ± 0.1**	–
Mixing	2nd	1.8	5	0.25/1.8	NA*/8.5 ± 0.2**	–
Collection	3rd	4.7	1	4.7/4.8	9.5 ± 0.2*/− 3.4 ± 0.1**	–
Aerated soft solid						
Compression	1st	9.1	5	0.9/10.0	NA*/23.4 ± 1.3**	11.0 ± 1.5
Bolus displacement	2nd	-	1	1.0/1.1	23.3 ± 0.1*/− 3.3 ± 0.1**	–
Shearing	3rd	3.3	7	0.4/3.6	NA*/28.9 ± 2.9**	17.1 ± 5.1
Collection	4th	1.1	1	1.1/1.2	23.3 ± 0.1*/− 3.3 ± 0.1**	–
Soft solid						
Compression	1st	5.8	3	1.0 / 6.2	NA*/22.7 ± 0.6**	9.8 ± 1.7
Bolus displacement	2nd	–	1	1.0 / 1.1	22.8 ± 0.2*/− 3.7 ± 0.1**	–
Shearing	3rd	1.2	5	0.2 / 1.7	NA*/25.7 ± 2.4**	12.1 ± 4.4
Collection	4th	1.3	1	1.3 / 1.4	22.8 ± 0.2**/− 3.7 ± 0.1**	–

Table 1. In vitro simulation of food oral processing. The parameters defined for in vitro food oral processing include the sequence of motions, the number of motions required to replicate the dominant action, the time allocated per motion and the total duration of the dominant action (based on TDM data and US recordings), the pressures exerted on the tongue (including both frontal (*) and lateral values (**)), and the palatal pressure recorded during the stages of multiple compressions or shear against the hard palate. Average data are presented alongside their respective standard deviations. To ensure reliability, a minimum of three experiments were conducted per food type. In instances denoted as "NA" (No Action), no specific motion is performed. The pressures applied by the tongue and against palate are in line with those observed in previous clinical studies, particularly in the context of consuming jellies with varying levels of hardness, spanning from soft (~ 5 kPa) to hard (< 40 kPa)[43]. The "time per motion" refers to the duration specified in the User LabView interface, which is based on the TDM profiles and FOP times extracted from US recordings. On the other hand, the "total time" encompasses not only the time required for inflation and deflation of the artificial tongue but also the cumulative duration of all motions applied. It is important to note the distinction between "Food displacement" and "Bolus displacement". In the former, the frontal air chamber remains uninflated, whereas in the latter, the frontal air chamber is fully inflated, akin to the "Collection" action. This ensures complete transportation of the food bolus from the frontal to the mid part of the oral cavity, facilitating further transformation during subsequent shearing actions.

- Food bolus mixing. The artificial tongue mirrors this action using an asymmetrical dome-like shape, alternating inflation and deflation in the lateral chambers to guide the movement of food from one side of the artificial oral cavity to the other (Fig. 3c, ii–iv). The sagittal view (Fig. 3c, iv) illustrates symmetrical inflation in both lateral chambers.
- Food bolus shearing. The artificial tongue replicates this phenomenon using an asymmetrical dome-like shape, similar to the shape employed for mixing but with increased pressure. This adjustment ensures proper contact between the tongue and hard palate, inducing complex shear within the food product (Fig. 3d, ii–iv). The sagittal view (Fig. 3d, iv) demonstrates symmetrical inflation in both lateral chambers.
- Final bolus collection. At the end of the in vitro sequence, the artificial tongue replicates Collection by inflating the frontal air chamber slightly to gently squeeze the food bolus, ensuring that any dispersed bolus in the frontal part of the oral cavity is displaced to the posterior part. Simultaneously, both lateral chambers deflate, creating a depression-like shape to contain the ready-to-swallow in vitro food bolus for final collection and further characterisation (Fig. 3e, ii–iii).

As detailed in "Materials and Methods", meticulous attention was given to crafting the pneumatic artificial tongue to emulate the mechanical properties, wettability, and surface papillae of the human tongue. To simulate the oral salivary coating initially present in the human mouth, 0.28 mL of water was used before each experimental run. In this initial phase, water is chosen to prevent any transformation of the food product by salivary enzymes prior to initiating the in vitro sequence (food products are allowed to rest inside the closed artificial oral cavity for 30 s to temper the system at 37 °C). The temperature of the food products was also adjusted before commencing the in vitro sequence. Freshly collected human saliva, with collection details outlined in "Materials and methods", is employed for in vitro simulation at a flow rate of 10 mL/min for all products, based on the in vivo data depicted in Fig. 1. The stages involved in the in vitro transformation of the model foods, including timing, actions performed, and applied pressure, are meticulously tailored to suit each type of food. This is achieved through a successive iterative comparison process between the in vitro and in vivo boli until their properties align accurately. All applied pressures are documented in Table 1, encompassing pressures exerted by the tongue against the hard palate to compress and shear the food bolus ("Palatal pressures"). It is intriguing to observe that

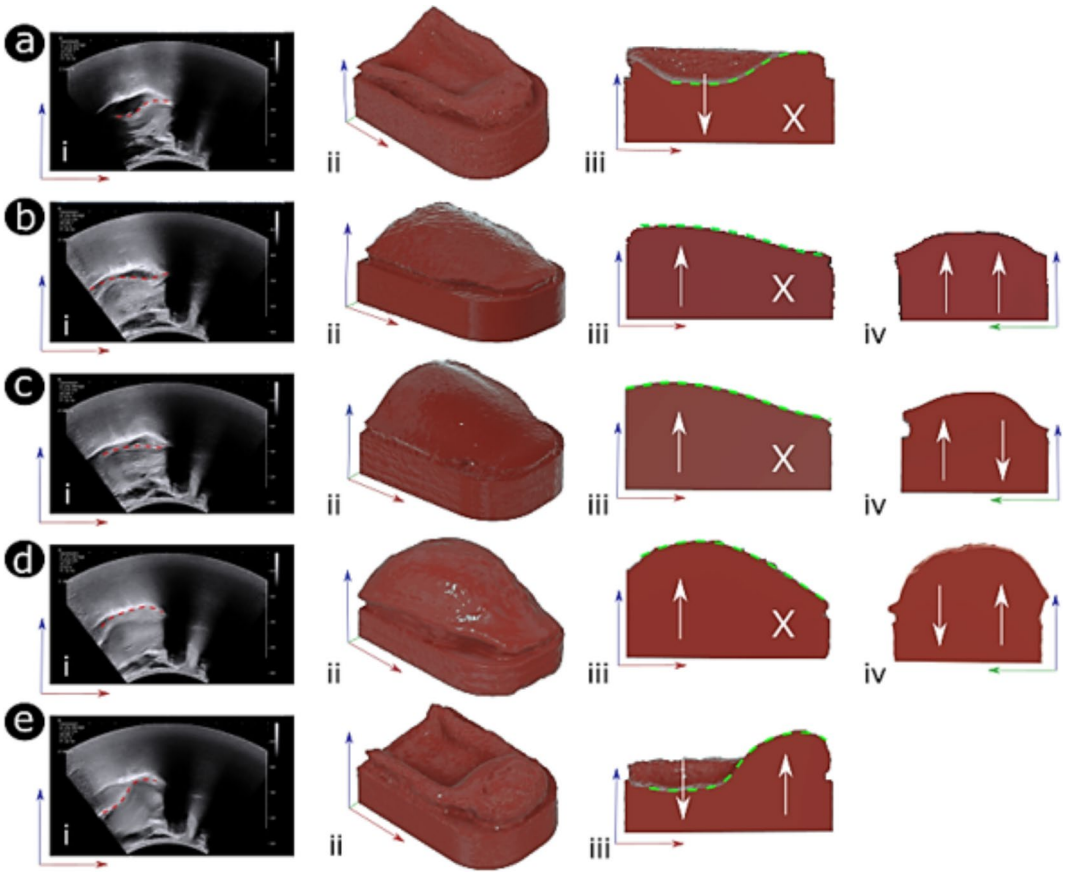

Fig. 3. Primary tongue actions mimicked during food oral processing. Coronal plane US images (i) along with their corresponding image-based 3D reconstructions (ii–iv) of the artificial tongue for each dominant motion. Initial isometric views (ii) aid in visualising tongue movements, followed by coronal (iii) and, if necessary, sagittal views (iv) to elucidate the shape of the artificial tongue. White arrows and X symbol denote the inflation/deflation or no-actioned states of tongue air chambers. Dashed lines, highlighted in red (US images) and green (3D reconstructions), qualitatively illustrate the mimicked shape. In the simulated oral environment, tongue mobility is constrained. In the initial phase of VL oral processing (**a**), the tongue transports the liquid from the frontal to the mid part of the oral cavity by slightly elevating the tip and depressing the tongue body (i). The artificial tongue replicates this action with a depression-like shape (ii–iii), maintaining the frontal air chamber with no action while the lateral chambers deflate. For both ASS and SS, oral processing begins with the tongue compressing the food against the hard palate (**b**.i). The artificial tongue mimics this action with a dome-like shape (ii), maintaining the frontal air chamber with no action while symmetrically inflating both lateral chambers (iii–iv). During mixing (**c**.i), the tongue moves the food product within the oral cavity to facilitate its mixing with saliva. The artificial tongue replicates this action with an asymmetrical dome-like shape (ii), alternating inflation and deflation in both lateral chambers (iii–iv). During shearing, evident tongue and hard palate contact produce a complex shear state (**d**.i). The artificial tongue mimics this with an asymmetrical dome-like shape (ii–iv), like the shape used for mixing, but with the tongue contacting against the hard palate to produce shear. At the end of oral processing, just before swallowing, food boli are collected in the back of the tongue (**e**.i). The artificial tongue mimics this action by inflating the frontal air chamber to squeeze slightly the food bolus while deflating both lateral chambers (ii–iii), producing a depression-like shape to contain the ready-to-swallow food bolus.

ASS, which displays the highest food resistance to initial deformation (firmness 99.3 ± 7.9 N.s, Fig. 1), resulted in elevated compression and shearing palatal pressures compared to SS, particularly noticeable during shearing. These pressures are consistent with those observed in vivo in previous clinical studies involving the consumption of jellies of varying hardness levels, ranging from soft (~ 5 kPa) to hard (< 40 kPa)[44]. The in vitro FOP times align with those outlined in Sect. 2.1, derived from US recordings ($n = 10$). A representative video of the motions of the artificial tongue is included as Supplementary Material.

Comparison between ready-to-swallow in vivo and in vitro food boli

Following the in vitro simulation sequences detailed in Sect. 2.4 and Table 1, in vitro boli of the model foods were collected at the "in vitro swallowing point" to evaluate their textural and rheological properties (Fig. 4), including firmness, cohesion work, adhesion work, maximum adhesive force, and shear viscosity data at specific

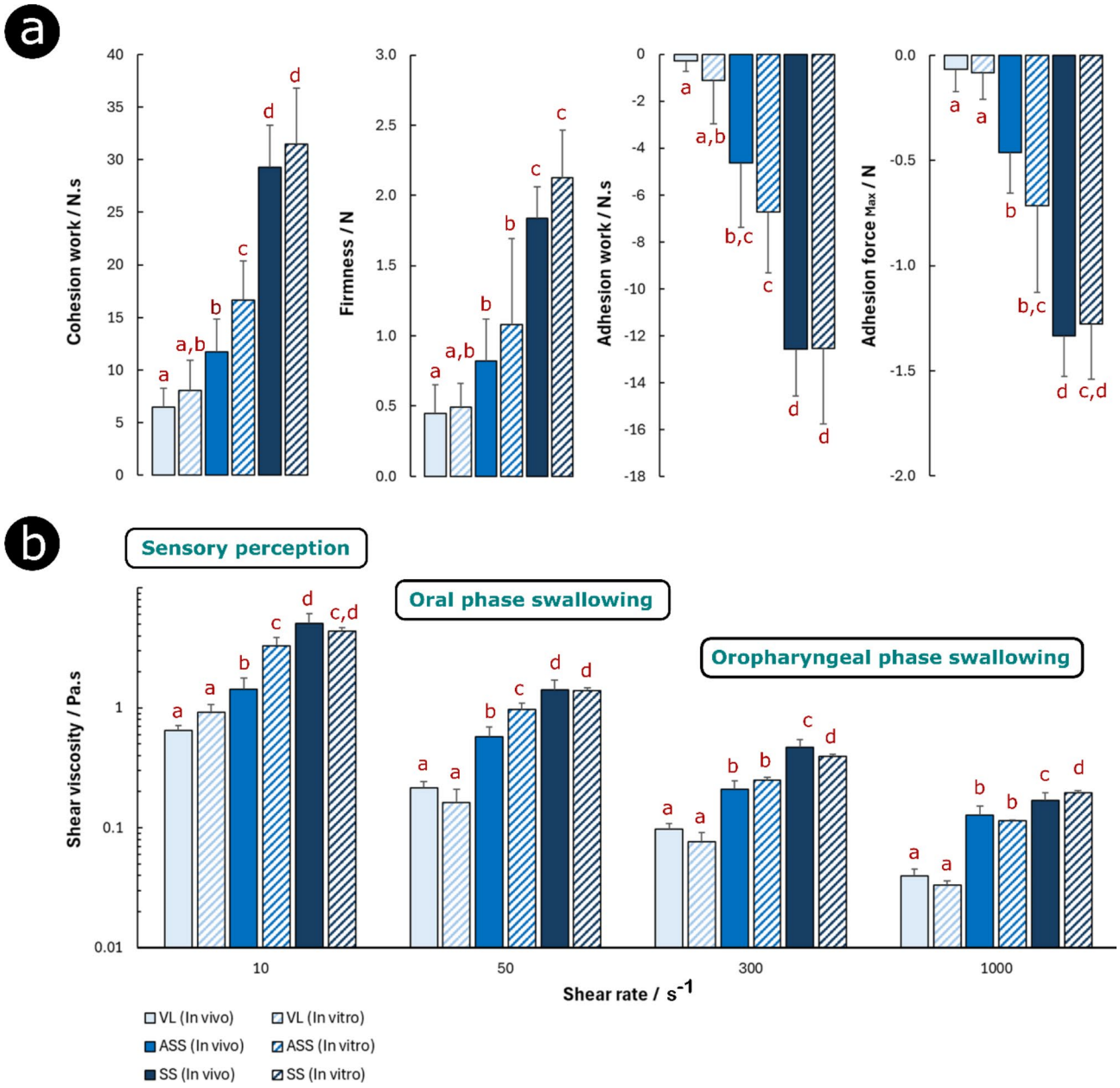

Fig. 4. Comparative analysis between ready-to-swallow food boli formed in vivo and those created in vitro. The parameters examined encompassed textural attributes (**a**), including firmness, cohesion work, adhesion work, and maximum adhesive force, along with shear viscosity data (**b**) at relevant shear rates, specifically those associated with sensory perception (10 s^{-1}), oral (50 s^{-1}) and oropharyngeal phases of swallowing (300–1000 s^{-1}). Additional parameters such as the food-to-saliva ratio (H_w), representing the ratio of saliva to the wet food sample, are provided in the Supplementary Information; no statistically significant differences between H_w values of in vivo and in vitro boli (refer to Supplementary Table SI.2). In vivo food boli underwent three repetitions across three different panellists ($n = 3 \times 3$), while in vitro food boli were subjected to at least three repetitions. The textural attributes and shear viscosities of the in vitro food boli closely mirrored those observed in ready-to-swallow in vivo boli for the model foods (Viscous Liquid (VL), Aerated Soft Aolid (ASS), Soft Solid (SS)). However, slight significant differences were noted for the work of cohesion and shear viscosities at low shear rates for in vitro ASS boli, as well as the viscosities of SS boli at oropharyngeal-relevant shear rates. Letters are used to represent statistical disparities among datasets.

shear rates relevant to texture perception (10 s^{-1}), oral (50 s^{-1}) and oropharyngeal phases of swallowing (300–1000 s^{-1})[40]. Additionally, parameters such as the food-to-saliva ratio (H_w) were analysed yet no statistical differences were observed between in vivo and in vitro data. ANOVA analysis is included in Table SI.2.

Similarly to what occurred during in vivo food oral processing, all textural and rheological properties of the formed food boli in vitro underwent significant modifications compared to the original characteristics of

the model foods. In fact, the textural attributes and shear viscosities of the in vitro food boli closely mirrored those observed in vivo. For VL, no significant differences were observed for any of the parameters analysed, indicating the successful creation of in vitro boli of the viscous liquid. All adhesive and cohesive properties were closely mimicked, suggesting its suitability for swallowing. Moreover, shear viscosities at oral and pharyngeal relevant shear rates were faithfully reproduced. Regarding ASS, all textural characteristics of in vivo boli were closely reproduced, except for cohesion work, which exhibited minimal statistical differences ($p = 0.049$). Some differences between in vivo and in vitro boli were also observed in viscosity data: while ASS bolus viscosities were accurately mimicked at oropharyngeal-like shear rate conditions, viscosities at lower shear rates, relevant to oral conditions, showed significant differences ($p \leq 0.001$). Finally, for SS, all textural properties of in vivo food boli were closely mimicked. Regarding viscosity data, viscosities at low shear rates were faithfully reproduced, yet some statistical differences were observed at higher shear rates ($p = 0.037$ and $p = 0.046$ at 300 s^{-1} and 1000 s^{-1}).

Discussion

During food consumption, oral processing involves mechanical and chemical actions essential for efficient swallowing, digestion, and nutrient absorption, and sensory experiences like taste, texture, and aroma perception[45]. Given that oral processing varies significantly based on the characteristics of the ingested food[27], this study examined three model foods: a viscous liquid, an aerated soft solid, and a soft solid.

In vivo, food is initially compressed by the tongue against the hard palate for texture recognition and determining further oral strategies[46]. Soft foods use tongue-palate actions for bolus formation, while harder foods require mastication. Sensory evaluations show tongue-palate compression for foods with a fracture force ≤ 15 N and mastication for those > 20 N[28]. Our model foods, with firmness below 10 N (Fig. 1), likely rely only on tongue dynamics for oral processing. This assumption is supported by the TDM profiles (Fig. 2), where mastication was not required among the panellists. A quasi-linear correlation between textural factors and compression duration ("Estimated in vivo time," Table 1) is also observed (Supplementary Fig. SI.2).

ASS, the hardest with the lowest water content—as observed for other type of foods[47] required the longest compression, followed by SS. Both VL and ASS showed smooth TDM compression profiles, while the SS had a two-stage compression period with significant shearing in the second stage, possibly indicative of the need to break down gel pieces to facilitate bolus formation. Shearing periods for ASS occurred post-compression, unlike the simultaneous shearing for SS.

The initial mechanical characteristics of food are crucial for determining the path of oral processing and bolus formation, but other textural properties, like adhesion, may also play a significant role in shaping the dynamics of food processing[48]. For instance, ASS, distinguished by its stickiness, exhibited over twice the adhesion work and force compared to other model foods. Notably, ASS uniquely displayed two marked swallowing stages, separated by a bolus collection phase, a phenomenon corroborated by the US recordings, where 5 out of 10 panellists engaged in a partial swallow. This behaviour may be attributed to its stickiness and complex aerated texture[49].

Achieving a harmonious balance between the adhesive and cohesive properties of the food bolus is crucial for swallowing[25,26]. All foods underwent substantial modifications in both textural and rheological properties during oral processing, as discussed in Sect. 2.1 and 2.2. In vivo boli of VL and ASS exhibited drastic reductions in their textural parameters: more than 80% of reduction for firmness and cohesion work, and 90% for adhesive properties. The resistance to flow of the in vivo boli at the orally relevant shear rate (50 s^{-1}) also displayed notable differences, with the most significant decrease observed for VL (91% reduction). Starch content and the salivary dilution effect (ratio of ~ 0.2) likely contributed to these changes. Salivary enzymes could further affect food transformation, particularly for semi-solid products where liquid characteristics may facilitate starch-enzyme interactions, drastically reducing viscosity. In contrast, solid foods with complex structures have limited interactions until they break down into smaller pieces.

Similarly to in vivo oral processing, in vitro food boli underwent significant modifications compared to the original model foods. The textural and rheological properties of the in vitro boli closely mirrored those of observed in ready-to-swallow in vivo boli (Fig. 4), achieving a similar adhesive/cohesive balance suitable for swallowing. The only exception was the in vitro ASS bolus, which showed minimal statistical differences in cohesion work. This may be attributed to its lactic esters of mono- and diglycerides of fatty acids emulsifier, which could be more temperature-sensitive than the soy lecithin and carrageenan in the other foods. Although the in vitro system incorporates a heating stage at the bottom part, the lack of temperature control around the translucid artificial cavity, unlike the human mouth, could account for these slight differences observed between in vivo and in vitro boli.

Replicating the rheological properties of in vitro boli is also important, as these can influence oral lubrication and sensory perception[50], as well as the later stage of swallowing[51]. The swallowing process encompasses a wide range of shear rates, ranging from 50 s^{-1}, associated with the oral phase, up to 1000 s^{-1}, associated with the oropharyngeal phase of swallowing[40]. The artificial mouth introduced in this study successfully reproduces the shear viscosity of in vivo boli of the VL across the full range of oral perception and swallowing (10–1000 s^{-1}), as well as the shear viscosity of ASS boli at oropharyngeal shear rates (300–1000 s^{-1}). However, the shear viscosity of in vitro ASS boli is slightly higher under orally relevant conditions, likely due to incomplete melting of the fatty compounds because of temperature control limitations. On the other hand, in vitro SS boli replicate in vivo viscosities at low shear rates (10–50 s^{-1}), with minimal differences at higher shear rates (1000 s^{-1}).

This pioneering artificial mouth marks a breakthrough in the field of food oral processing research, offering unprecedented realism in replicating the intra-oral transformation of foods. This extraordinary capability opens exciting new avenues for investigating food oral perception, lubrication, and swallowing in vitro, promising substantial advancements in our comprehension of these intricate processes.

Limitations

The limitations of this study are discussed in this paragraph. Water was used instead of saliva to replicate the initial oral cavity lubrication and prevent any alterations of the rheological properties of the model foods before in vitro processing. Additionally, the lack of temperature control around the translucent oral cavity of the in vitro system, unlike the human mouth, may affect food processing, especially for temperature-sensitive foods.

Conclusions

In this work, we introduce a pioneering 3D biomimetic artificial mouth featuring a pneumatic multi-degree-of-freedom artificial tongue. Designed to emulate the mechanical characteristics, wettability, surface papillae, and lifelike motions of the human tongue, this artificial mouth faithfully replicates the oral processing of different foods, including viscous liquids, aerated and soft solid foods. This device successfully produces in vitro food boli with a delicate balance between adhesive and cohesive properties like those observed in vivo, while also accurately mirroring rheological properties across a wide range of shear rates relevant for oral perception and swallowing. The artificial mouth presents unprecedented opportunities for studying the dynamics of food transformation in the oral cavity, promising enhancements in palatability and functionality of custom foods tailored to individual health needs, particularly for older populations.

Experimental section

Model foods

Three dairy chocolate-based foods of differing textural attributes were chosen, including a viscous liquid (Crème dessert, Danette, France), an aerated soft solid (Mousse Chocolat, Danette, France) and a soft solid (gel-like consistency) (Fondant Cacao, Les 2 Vaches, France). Their compositional details are included in Supplementary Table SI.3. According to manufacturer information, starch is present in all products.

Determination of water and food insalivation ratio

The amount of saliva secreted during oral processing were assessed using a reduced group of healthy adult volunteers ($n=3$, aged 30 ± 2 years). The volunteers took a teaspoon of the specific product and engaged in their usual oral processing routine. Prior to conducting the tests, these products were allowed to reach room temperature for tempering. Upon completing oral processing and reaching the point of swallowing, the formed boli were spat into a container. To recover any oral residues left by the product, 5 mL of mineral water (Vittel, France) were used. After oral rinsing, this water alongside food residues were spat into a separate container. During food oral processing, time was recorded, to estimate the stimulated salivary flow rate of each volunteer. Tests were performed at least three times per volunteer ($n=3\times3$). The ratio of saliva added in the bolus was determined respect to wet food sample (H_w)[52]. Dry matter content was determined after dehydration in an oven at 105 °C for 24 h.

Textural and rheological characterization

A texture analyzer TAXT Plus (Stable Micro Systems Ltd., Surrey, United Kingdom) with a Back Extrusion Test (BET) rig (details provided in Supplementary Fig. SI.3a) was used to determine from the force–time graph textural properties of the food samples and boli, including firmness, cohesion work, adhesion work, and maximum adhesion force (Supplementary Fig. SI.3b). Approximately 15 mL of the food sample/bolus were placed in a standard sample container with a capacity of 40 mL (28 mm inner diameter), in a way to avoid air entering and providing a smooth upper surface. The samples were compressed by a Plexi piston of 25 mm diameter, providing an extrusion of the product upward between the walls and edges of the piston. For measuring the force produced by the samples, the 5 g load cell was used. The parameters of the study were a speed rate of 1 mm/s and a depth of insertion of 20 mm. Three replicate analyses were carried out at a room temperature (20 °C) for each sample, providing the same conditions for each measurement and per each volunteer.

Shear viscosity of food samples and boli (right after collection) were assessed with a Modular Compact Rheometer 702 (Anton Paar GmbH, Graz, Austria) at 20 °C, using a parallel-plate geometry (PP25) with a rough surface for the model foods, and a geometry CC25 for in vivo and in vitro food boli. Shear viscosity was evaluated by steady shear tests in a range of shear rates between 1 and 1000 reciprocal seconds.

Temporal dominance of motions (TDM) and ultrasounds recordings

The study was carried out in accordance with the regulations of the Ethics Committee for Research (CER) of the Université Paris-Saclay (reference CER-Paris-Saclay-2022-085). All methods were performed in accordance with the relevant guidelines and regulations of the Université Paris-Saclay. For conducting sensory perception tests of oral motions, model food samples were transferred and presented on plastic trays with teaspoons with sampling so that the teaspoon was filled before testing. Due to their differing composition (water content, physical state, aeration grade), the amount of food on each teaspoon was not standardised by either volume or weight but represented a standardised scoop of the product that would likely be made in free consumption. This resulted in the mass of product contained in the spoons of approximately 10 g for poorly aerated products and 6 g for aerated products. The spoons were labelled with random 3-digit numbers that were predetermined. Commercial mineral water (Evian, France) and flavourless crackers (Lu biscuit, France) were used for mouth rinsing and offsetting texture cues during consumption respectively. Foods were stored at 3 °C in a fridge cold room, being later tempered at room temperature before testing.

A total of sixteen panellists ($n=16$) were recruited for 6 testing sessions of 30 min. Written informed consent was obtained from each subject after explanation of the aim and methodology of the study. Sensory tests were done on touch tablets where the testing procedures were programmed using FIZZ software (Biosystemes,

France). The procedure involves presenting the panellists with a list of six oral motions: compression, shearing, mixing, and bolus collection for the tongue, mastication for the teeth, and swallowing (detailed in Table 2). Panellists are then prompted to select the dominant attribute throughout food oral processing. The data obtained are normalised over time, ranging from 0% (when the product is introduced into the mouth) to 100% (the end of oral movements after swallowing). Temporal Dominance of Motions (TDM) analysis[42], based on the well-known Temporal Dominance of Sensations (TDS) method, was employed during consumption of the three model foods. Each product undergoes two repetitions. The normalised data are plotted as curves showing the temporal variations in the citation rate for the different attributes, expressed as a percentage of the 2×16 experiments conducted for each product. A curve smoothing function is applied to the data using software to facilitate visualisation.

In addition to sensory evaluations, US imaging measurements were conducted on a total of 10 out of the 16 panellists. The objective of these proof-of-concept acquisitions was evaluating the potential of US imaging for monitoring the motions of the tongue all along the oral processing of the different food products. Acquisitions were conducted with the ultrasound platform Aixplorer (Supersonic Imagine, France), equipped with a convex probe (XC6-1, Supersonic Imagine, France) composed of 192 elements and operating on a bandwidth equal to 1–6 MHz. This probe was mounted on a dedicated headset (UltraFit, Articulate Instruments, U.K.) designed to allow a reproducible positioning of the US probe under the chin of the volunteers. Once the probe was in place on the volunteer, an automatic time gain compensation function was applied to optimise the quality of the images obtained, in particular to adapt to the variability of the attenuation of the ultrasound waves, influenced by inter individual variations of anatomy. Ultrasound acquisitions were conducted all along food oral processing for the three food products, and recorded under the form of videos, with a resolution of 1296 by 972 pixels and a frame rate of 32 Hz. Representative US recordings demonstrating each sequence performed are included as Supplementary Material.

Human saliva collection

Saliva was obtained from two healthy adult individuals (32 ± 2 years old) who abstained from consuming any foods or drinks (except water) for a minimum of 2 h prior to collection. Right after collecting the saliva sample, it was heated at 37 °C and used for simulating in vitro oral processing without undergoing centrifugation. Despite centrifugation does not affect the lubricating characteristics of saliva[53], it does effectively remove high molecular weight proteins like mucins that are frequently associated with the distinctive rheological properties of saliva, including viscosity, elasticity, stickiness, and its ability to retain water under relevant oral conditions[54].

3D biomimetic oral cavity

The artificial oral cavity is meticulously crafted, drawing upon detailed 320-row area detector computed tomography scans of a healthy adult oral cavity[55] (Fig. 5a). The use of CT images of adult volunteers is approved by Fujita Health University Ethics Review Committee (reference number: HM18-431). Considering a surface area of the palatal area of the artificial oral cavity of ~ 2272 mm^2, aligning well with data reported in other in vivo studies[56], along with other the regions encompassing the lingual teeth area and the top surface of the non-inflated artificial tongue, the total inner area of the artificial mouth is approximately 6394 mm^2. The artificial oral cavity (Fig. 5b) is equipped with a pressure sensor (HDP502, HHAT, China) to monitor and record the palatal pressure during food oral processing, and four salivary inlets to control and distribute the salivary fluid across the oral cavity. The system also features a soft actuator mimicking the human tongue, a heating stage (50×25 mm) with a temperature sensor that automatically regulate the oral temperature at 37 °C, the respective holders for the tongue and the oral cavity, and a LED light panel that will be used for facilitating video recording.

Artificial tongue

The pneumatic soft robotic actuator (Fig. 5c.i), designed to resemble the human tongue, possesses external dimensions that align with the artificial oral cavity. To create the artificial tongue, a platinum-catalysed silicone rubber (Ecoflex 00–30, Smooth-on Inc., U.S.A)[63] of hardness (77 ± 9 kPa[57]), comparable to that of the human tongue (12 kPa at rest and 122 kPa in tension state[28]), was employed. The silicone rubber is prepared following the guidelines provided by the supplier. The 3D tongue moulds were manufactured in PLA (MakerBot Replicator 2). Further information regarding its manufacturing process can be found in Supplementary Fig. SI.4a. As the mechanics of food perception and transport are significantly influenced by the interplay of oral friction, particularly influenced by the densely populated micropapillae[58], the upper surface of the soft actuator was biomimetically texturized (Fig. 5c.ii) based on in vivo data[59]: filiform (density 160.0 ± 30.0 per 10^{-4} m^2, diameter 355.0 ± 40.0 µm, and height 195.0 ± 6.5 µm) and fungiform papillae (density 13.5 ± 1.5 per 10^{-4}

Attributes	Definition
Compression	The food is compressed as the tongue rises and comes into contact with the hard palate
Shearing	Shearing of the food occurs through the movements between the tongue and the hard palate
Mixing	The tongue aids in mixing the food, promoting its dilution with saliva
Collection	Collecting of fragments and remnants through various tongue movements
Mastication	Employing the teeth to masticate food
Swallowing	The food bolus is compressed, moving toward the rear of the oral cavity in preparation for swallowing, and then swallowed

Table 2. Attributes used for the temporal dominance of motions judgments.

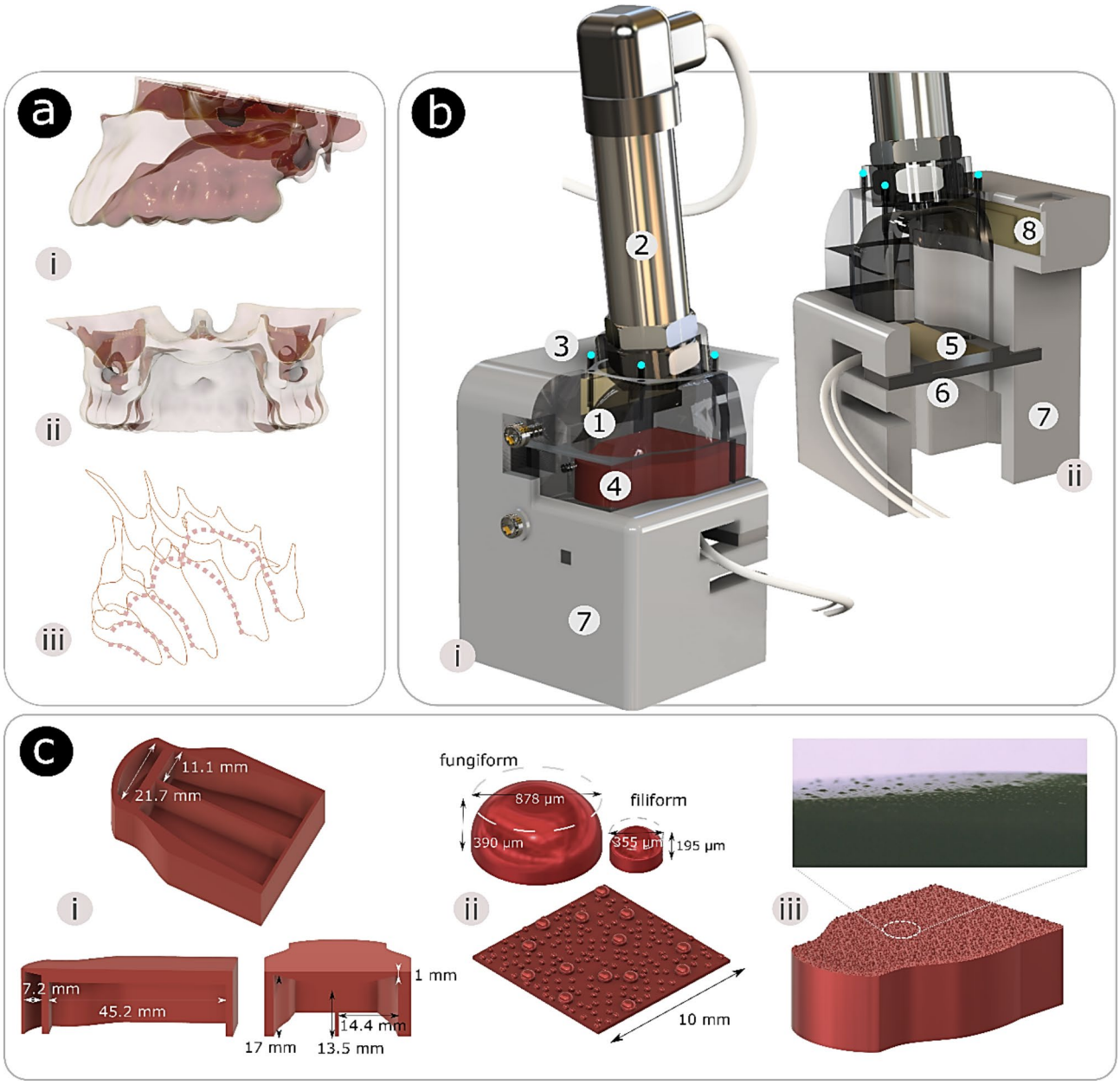

Fig. 5. 3D biomimetic artificial mouth. A 320-row area detector computed tomography scan (**a**) of a healthy adult used for the design of the artificial oral cavity. This included coronal (i) and sagittal (ii) views, along with a representative sectional profile (dashed lines) used for reconstructing the artificial cavity through Loft command of Fusion360. The 3D CAD design (**b**) of the in vitro system comprises an artificial oral cavity (1), equipped with a pressure sensor (2) to monitor palatal pressure during food oral processing, and four salivary inlets (3) (highlighted by blue points to facilitate visualisation) to control and distribute the salivary fluid. The system also features a soft actuator (4) mimicking the human tongue, a heating stage (5) (50 × 25 mm) with a temperature sensor, a tongue/heating stage holder (6), an oral cavity holder (7), and a LED light panel (8) used for video recording. The centre of the pressure sensor is positioned approximately 35 mm from the frontal wall and 22 mm from the side wall of the artificial oral cavity. The artificial tongue design is also presented[62] (**c**), showcasing the soft actuator dimensions in top, lateral, and posterior sectional views (i). The top surface texturization (ii) includes the crafted 3D CAD model of artificial papillae, designed meticulously based on average in vivo data (details provided in "Materials and methods"). This model, with a surface area of 10 × 10 mm, incorporates a randomised distribution of both fungiform and filiform papillae. The resulting model is applied to the top surface of the soft actuator (iii), offering a captivating snapshot of the designed surface pattern captured by a digital camera at ×50 magnification.

m^2, diameter 878.0 ± 97.0 µm, and height 390.0 ± 72.0 µm). While fungiform papillae exhibit dome-shaped structures surrounded by an array of filiform papillae, the filiform papillae manifest themselves as clusters of slender cylinders, approximately half the width and height of individual fungiform papillae[59]. The biomimetic tongue-like surface was designed using Fusion 360 (Autodesk, Inc., France), generating a model surface pattern (10 × 10 mm) with a random spatial distribution of filiform and fungiform papillae, avoiding overlapping. The surface texturing mould was 3D printed in resin (ElegooMars 2P) to mould-cast the upper surface of the tongue.

The control algorithm responsible for orchestrating the inflation and deflation of the air chambers was implemented in LabVIEW (National Instruments), using an Arduino Uno board (Arduino AG, Chiasso, Switzerland) for precise control over the pumping sequence. Through a pneumatic system, the soft tongue deformation is regulated by finely adjusted solenoid valves and a rotary vane vacuum pump. To monitor and maintain optimal air pressure within the lines, pressure transducers are employed, with the maximum inflation pressures being adjusted as required using needle valves. Further information of the control system can be found in Supplementary Fig. SI.4b.

Initial salivary-like coating of the artificial mouth

In the human mouth, saliva is distributed across hard and soft oral tissues, forming a delicate salivary film. Considering the surface area of the artificial mouth and an average salivary coating thickness of ~ 43 µm, derived from in vivo data[56], the initial amount of saliva required for an accurate reproduction of the salivary coating is 0.28 mL. In this case, deionised water was used to avoid chemical transformation that could happen with food while the system is heating up, before triggering the oral processing sequence. The amount of water was applicated using a spray bottle, with the precise amount being calibrated.

Wetting properties of the artificial mouth

Surface wettability was evaluated through contact angle measurements conducted on a water droplet (10 µL) at equilibrium, employing the sessile drop technique. The temporal evolution of the contact angle was captured by a high-speed camera (model ac A2040-120 µm, Basler, Germany), and data processing was conducted using ImageJ. To reduce Ecoflex 00–30 hydrophobicity (initially 85.2 ± 4.8°), a surfactant (Span 80, 0.5 wt%) was introduced[57,63], resulting in a remarkable wettability improvement (34.4 ± 3.8°). The addition of Span 80 at this concentration does not affect the tensile response of Ecoflex 00–30[57]. Surface texturing of the artificial tongue modified its wetting properties, reducing wettability by a factor of two (68.1 ± 3.8°). Comparatively, the wetting properties of the artificial oral cavity material (Veroclear, Sculpteo, France) exhibited contact angles of 82.5 ± 2.9°. Notably, these data align with those reported for oral tissues, approximately 77° for pig tongues[59] and 72°–79° for human gingival surfaces[60].

Image-based 3D tongue reconstruction

A Canon EOS 750D camera was employed to capture 360° images of the artificial tongue simulating the primary motions relevant to reproduce oral processing in vitro. One picture was taken every 10° of rotation in a ScanCube 308 chamber (ScanCube, France). Subsequently, image-based 3D tongue reconstruction models were generated using AgiSoft software (Agisoft LLC, Russia).

Statistical analysis

One-way ANOVA analysis was conducted to assess statistical differences between datasets. When *p*-value corresponding to the *F*-statistic of one-way ANOVA was lower than 0.05, suggesting that one or more pairs of treatments are significantly different, post-hoc Tukey's HSD test was applied.

Data availability

The data used to support the findings of this study are available from the corresponding author upon request.

Received: 3 July 2024; Accepted: 19 September 2024
Published online: 15 October 2024

References

1. United Nations. World Population Prospects 2019: Highlights. June 2019. Retrieved from (2019). https://population.un.org/wpp#UNPopulation. .
2. United Nations, Department of Economic and Social Affairs, Population Division. World Population Ageing 2019: Highlights (ST/ESA/SER.A/430). (2019).
3. World Health Assembly. The Global strategy and action plan on ageing and health 2016–2020: towards a world in which everyone can live a long and healthy life. World Health Organization. Retrieved from (2016). https://iris.who.int/handle/10665/252783
4. Clegg, M. E. et al. The Food4Years Ageing Network: improving foods and diets as a strategy for supporting quality of life, independence and healthspan in older adults. *Nutr. Bull.***48** (1), 124–133. https://doi.org/10.1111/nbu.12599 (2023).
5. Smith, R., Clegg, M. E. & Methven, L. Review of protein intake and suitability of foods for protein-fortification in older adults in the UK. *Crit. Rev. Food Sci. Nutr.* 1–18. https://doi.org/10.1080/10408398.2022.2137777 (2022).
6. van der Pols-Vijlbrief, R., Wijnhoven, H. A., Schaap, L. A., Terwee, C. B. & Visser, M. Determinants of protein-energy malnutrition in community-dwelling older adults: a systematic review of observational studies. *Ageing Res. Rev.* **18**, 112–131. https://doi.org/10.1016/j.arr.2014.09.001 (2014).
7. Alia, S. et al. The influence of age and oral health on taste perception in older adults: a case-control study. *Nutrients.* **13** (11), 4166. https://doi.org/10.3390/nu13114166 (2021).
8. Doty, R. L. & Kamath, V. The influences of age on olfaction: a review. *Front. Psychol.* **5**, 20. https://doi.org/10.3389/fpsyg.2014.00020 (2014).
9. Lin, C. S. Functional adaptation of oromotor functions and aging: a focused review of the evidence from brain neuroimaging research. *Front. Aging Neurosci.* **11**, 354. https://doi.org/10.3389/fnagi.2019.00354 (2020).

10. Withers, C., Gosney, M. A. & Methven, L. Perception of thickness, mouth coating and mouth drying of dairy beverages by younger and older volunteers. *J. Sens. Stud.* **28** (3), 230–237. https://doi.org/10.1111/joss.12039 (2013).
11. Hall, G. & Wendin, K. Sensory design of foods for the elderly. *Ann. Nutr. Metab.* **52** (Suppl. 1), 25–28. https://doi.org/10.1159/000115344 (2008).
12. Thiyagalingam, S., Kulinski, A. E., Thorsteinsdottir, B., Shindelar, K. L. & Takahashi, P. Y. Dysphagia in older adults. *Mayo Clin. Proc.* **96**(2), 488–497. https://doi.org/10.1016/j.mayocp.2020.08.001 (2021).
13. Dibello, V. et al. Oral frailty and its determinants in older age: a systematic review. *Lancet Healthy Longev.* **2** (8), e507–e520. https://doi.org/10.1016/S2666-7568(21)00143-4 (2021).
14. Ikebe, K. et al. Association of masticatory performance with age, posterior occlusal contacts, occlusal force, and salivary flow in older adults. *Int. J. Prosthodont.* **19** (5), 475–481 (2006).
15. Peyron, M. A., Blanc, O., Lund, J. P. & Woda, A. Influence of age on adaptability of human mastication. *J. Neurophysiol.* **92** (2), 773–779. https://doi.org/10.1152/jn.01122.2003 (2004).
16. de Sire, A. et al. Sarcopenic dysphagia, malnutrition, and oral frailty in elderly: a comprehensive review. *Nutrients*. **14** (5), 982. https://doi.org/10.3390/nu14050982 (2022).
17. Clegg, M. E. & Williams, E. A. Optimizing nutrition in older people. *Maturitas*. **112**, 34–38. https://doi.org/10.1016/j.maturitas.2018.04.001 (2018).
18. Chambers, L. Food texture and the satiety cascade. *Nutr. Bull.* **41** (3), 277–282. https://doi.org/10.1111/nbu.12221 (2016).
19. Norton, V., Lovegrove, J. A., Tindall, M., Garcia, J. R. & Lignou, S. Fibre4life: investigating older adults dietary fibre preferences and the role of targeted educational materials on modulating future dietary fibre intake. *Appetite*. **192**, 107109. https://doi.org/10.1016/j.appet.2023.107109 (2024).
20. Engelen, L. et al. A comparison of the effects of added saliva, alpha-amylase and water on texture perception in semisolids. *Physiol. Behav.* **78** (4–5), 805–811. https://doi.org/10.1016/S0031-9384(03)00083-0 (2003).
21. Mosca, A. C. & Chen, J. Food-saliva interactions: mechanisms and implications. *Trends Food Sci. Technol.* **66**, 125–134. https://doi.org/10.1016/j.tifs.2017.06.005 (2017).
22. He, Y., Wang, X. & Chen, J. *Annu. Rev. Food Sci. Technol.* **13**, 167–192. https://doi.org/10.1146/annurev-food-052720-103054 (2022).
23. Tonni, I. et al. The influence of food hardness on the physiological parameters of mastication: a systematic review. *Arch. Oral Biol.* **120**, 104903. https://doi.org/10.1016/j.archoralbio.2020.104903 (2020).
24. Pereira, L. J., Gavião, M. B., Engelen, L. & Van der Bilt, A. Mastication and swallowing: influence of fluid addition to foods. *J. Appl. Oral Sci.* **15** (1), 55–60. https://doi.org/10.1590/s1678-77572007000100012 (2007).
25. Loret, C. et al. Physical and related sensory properties of a swallowable bolus. *Physiol. Behav.* **104** (5), 855–864. https://doi.org/10.1016/j.physbeh.2011.05.014 (2011).
26. Peyron, M. A. et al. Role of physical bolus properties as sensory inputs in the trigger of swallowing. *PLoS One*. **6** (6), e21167. https://doi.org/10.1371/journal.pone.0021167 (2011).
27. Bolhuis, D. P. & Forde, C. G. Application of food texture to moderate oral processing behaviors and energy intake. *Trends Food Sci. Technol.* **106**, 445–456. https://doi.org/10.1016/j.tifs.2020.10.021 (2020).
28. Ishihara, S. et al. Instrumental uniaxial compression test of gellan gels of various mechanical properties using artificial tongue and its comparison with human oral strategy for the first size reduction. *J. Texture Stud.* **45** (5), 354–366. https://doi.org/10.1111/jtxs.12080 (2014).
29. Hayashi, H. et al. Biomechanics of human tongue movement during bolus compression and swallowing. *J. Oral Sci.* **55** (3), 191–198. https://doi.org/10.2334/josnusd.55.191 (2013).
30. Alsanei, W. A., Chen, J. & Ding, R. Food oral breaking and the determining role of tongue muscle strength. *Food Res. Int.* **65**, 331–337. https://doi.org/10.1016/j.foodres.2014.11.039 (2014).
31. Alsanei, W. A. & Chen, J. Studies of the oral capabilities in relation to bolus manipulations and the ease of initiating bolus flow. *J. Texture Stud.* **45** (1), 1–12. https://doi.org/10.1111/jtxs.12041 (2014).
32. Machida, N. et al. Effects of aging and Sarcopenia on tongue pressure and jaw-opening force. *Geriatr. Gerontol. Int.* **17** (2), 295–301. https://doi.org/10.1111/ggi.12715 (2017).
33. Peyron, M. A. & Woda, A. An update about artificial mastication. *Curr. Opin. Food Sci.* **9**, 21–28. https://doi.org/10.1016/j.cofs.2016.03.006 (2016).
34. Zhang, X., Chen, J., Panda, S. & Benjamin, O. Feasibility analysis of a newly developed multifunctional mastication simulator. *Innov. Food Sci. Emerg. Technol.* **87**, 103393. https://doi.org/10.1016/j.ifset.2021.104147 (2023).
35. Ribes, S. et al. Oral impairments decrease the nutrient bioaccessibility of bread in the elderly. *Food Hydrocolloids.* **115**, 108202. https://doi.org/10.1016/j.foodhyd.2022.108202 (2022).
36. Avila-Sierra, A., Decerle, N., Ramaioli, M. & Peyron, M. A. Effect of salivary fluid characteristics on the physical features of in vitro bread bolus: from the absence of saliva to artificially simulated hypersalivation. *Food Res. Int.* **175**, 113753. https://doi.org/10.1016/j.foodres.2023.113753 (2023).
37. Park, J. W. et al. Effects of texture properties of semi-solid food on the sensory test for pharyngeal swallowing effort in the older adults. *BMC Geriatr.* **20**, 493. https://doi.org/10.1186/s12877-020-01890-4 (2020).
38. Soltanahmadi, S., Bryant, M. & Sarkar, A. Insights into the multiscale lubrication mechanism of edible phase change materials. *ACS Appl. Mater. Interfaces*. **15** (3), 3699–3712. https://doi.org/10.1021/acsami.2c13017 (2023).
39. Srivastava, R. et al. A new biomimetic set-up to understand the role of the kinematic, mechanical, and surface characteristics of the tongue in food oral tribological studies. *Food Hydrocolloids.* **115**, 106602. https://doi.org/10.1016/j.foodhyd.2021.106602 (2021).
40. Ross, A. I. V., Tyler, P., Borgognone, M. G. & Eriksen, B. M. Relationships between shear rheology and sensory attributes of hydrocolloid-thickened fluids designed to compensate for impairments in oral manipulation and swallowing. *J. Food Eng.* **263**, 123–131. https://doi.org/10.1016/j.jfoodeng.2019.05.040 (2019).
41. Lavoisier, A., Boudrag, S. & Ramaioli, M. Effect of α-amylase and pH on the rheological properties of thickened liquids containing starch in in vitro conditions relevant to oral processing and swallowing. *J. Texture Stud.* **53** (4), 550–557. https://doi.org/10.1111/jtxs.12693 (2022).
42. Saint-Eve, A., Mathieu, V., Mantelet, M., Morgenstern, M. P. & Souchon, I. Temporal Dominance of Motions: a new concept to enlighten the links between texture perceptions and oral processing. In *5th international conference on Food Oral Processing, 1st–4th July 2018, Nottingham, UK. Oral.*
43. Hiiemae, K. & Palmer, J. Food transport and bolus formation during complete feeding sequences on foods of different initial consistency. *Dysphagia*. **14**, 31–42. https://doi.org/10.1007/PL00009582 (1999).
44. Yokoyama, S. et al. Tongue pressure modulation for initial gel consistency in a different oral strategy. *PLoS One*. **9** (3), e91920. https://doi.org/10.1371/journal.pone.0091920 (2014).
45. Chen, J. Food oral processing: some important underpinning principles of eating and sensory perception. *Food Struct.* **1** (2), 91–105. https://doi.org/10.1016/j.foostr.2014.03.001 (2014).
46. Arai, E. & Yamada, Y. Effect of the texture of food on the masticatory process. *Jpn. J. Oral Biol.* **35**, 312–322 (1993).
47. Hennelly, P. J. et al. Increasing the moisture content of imitation cheese: effects on texture, rheology and microstructure. *Eur. Food Res. Technol.* **220**, 415–420. https://doi.org/10.1007/s00217-004-1097-9 (2005).
48. Kazemeini, S. M., Campos, D. P. & Rosenthal, A. J. Muscle activity during oral processing of sticky-cohesive foods. *Physiol. Behav.* **242**, 113580. https://doi.org/10.1016/j.physbeh.2021.113580 (2021).

49. Bikos, D. et al. Effect of micro-aeration on the mechanical behaviour of chocolates and implications for oral processing. *Food Funct.* **12** (11), 4864–4886. https://doi.org/10.1039/D1FO00045D (2021).
50. Sarkar, A. & Krop, E. M. Marrying oral tribology to sensory perception: a systematic review. *Curr. Opin. Food Sci.* **27**, 64–73. https://doi.org/10.1016/j.cofs.2019.05.007 (2019).
51. Marconati, M. & Ramaioli, M. The role of extensional rheology in the oral phase of swallowing: an in vitro study. *Food Funct.* **11** (5), 4363–4375. https://doi.org/10.1039/C9FO02327E (2020).
52. Drago, S. R. et al. Relationships between saliva and food bolus properties from model dairy products. *Food Hydrocoll.* **25** (4), 659–667. https://doi.org/10.1016/j.foodhyd.2010.07.024 (2011).
53. Zhang, Y. F., Zheng, J., Zheng, L. & Zhou, Z. R. Influence of centrifugation treatment on the lubricating properties of human whole saliva. *Biosurfa. Biotribol.* **2**, 95–101. https://doi.org/10.1016/j.bsbt.2016.09.001 (2016).
54. Sarkar, S. Human saliva and model saliva at bulk to adsorbed phases—similarities and differences. *Adv. Colloid Interface Sci.* **273**, 102034. https://doi.org/10.1016/j.cis.2019.102034 (2019).
55. Kobayashi, Y. et al. Velopharyngeal closure analysis using four-dimensional computed tomography: a pilot study of healthy volunteers and adult patients with cleft palate. *BMC Med. Imaging.* **19** (54). https://doi.org/10.1186/s12880-019-0350-4 (2019).
56. Assy, Z., Jager, D. H. J., Brand, H. S. & Bikker, F. J. Salivary film thickness and MUC5B levels at various intra-oral surfaces. *Clin. Oral Investig.* **27** (2), 859–869. https://doi.org/10.1007/s00784-022-04626-3 (2023).
57. Marconati, M. In vitro models for the formulation of easy-to-swallow products. PhD thesis, University of Surrey, U.K. (2019).
58. Lauga, E., Pipe, C. J. & Le Reverend, B. Sensing in the mouth: a model for filiform papillae as strain amplifiers. *Front. Phys.* **4**, 35. https://doi.org/10.3389/fphy.2016.00035 (2016).
59. Andablo-Reyes, E. et al. 3D biomimetic tongue-emulating surfaces for tribological applications. *ACS Appl. Mater. Interfaces.* **12** (44), 49371–49385. https://doi.org/10.1021/acsami.0c12925 (2020).
60. Van der Meia, H. C., White, D. J. & Busscher, H. J. On the wettability of soft tissues in the human oral cavity. *Arch. Oral Biol.* **49** (8), 671–673. https://doi.org/10.1016/j.archoralbio.2004.03.002 (2004).
61. Pineau, N. et al. Temporal dominance of sensations: construction of the TDS curves and comparison with time-intensity. *Food Qual. Prefer.* **20** (6), 450–455. https://doi.org/10.1016/j.foodqual.2009.04.005 (2009).
62. Avila-Sierra, A., Bugarin-Castillo, Y., Voisin, J., Mathieu, V. & Ramaioli, M. Toward a more realistic 3D biomimetic soft robotic tongue to investigate oral processing of semi-solid foods. In *Conference on Biomimetic and Biohybrid Systems* 131–140 (Springer Nature Switzerland, 2023).
63. Lavoisier, A. et al. A novel soft robotic pediatric in vitro swallowing device to gain insights into the swallowability of mini-tablets. *Int. J. Pharm.* **629**, 122369. https://doi.org/10.1016/j.ijpharm.2022.122369 (2022).

Acknowledgements

The authors ackowledge funding under the MSCA PF grant SENSINGTech Grant agreement ID: 101066647. A.A.S. thanks Maxime Grenier from INRAE UMR SayFood (Palaiseau, France) for his support with the image-based 3D reconstructions of the artificial tongue.

Author contributions

A.A.S., Y.B.C. and M.R. conceptualised and supervised the in vitro study and its experimental protocol. A.A.S. designed, developed, and optimised the in vitro system. J.B. designed and manufactured the pneumatic control system and electrical parts. M.G., A.S.E. and V.M. conceptualised and supervised the in vivo study and its experimental protocol. A.A.S and Y.B.C performed data extraction from the in vivo study and the characterisation of the model foods and boli. K.Y. provided the 320-row area detector computed tomography scans used for the design of the in vitro system. A.A.S. carried out statistics and prepared figures. A.A.S. wrote the main manuscript, with inputs from all authors. All authors reviewed the manuscript.

Declarations

Competing interests

The authors declare no competing interests.

Additional information

Supplementary Information The online version contains supplementary material available at https://doi.org/10.1038/s41598-024-73629-9.

Correspondence and requests for materials should be addressed to A.A.-S. or M.R.